Atmos. Chem. Phys. Discuss., https://doi.org/10.5194/acp-2018-880
Manuscript under review for journal Atmos. Chem. Phys.
Discussion started: 5 September 2018

Atmospheric Chemistry and Physics Discussions

Rapid SO_2 emission reductions significantly increase tropospheric ammonia concentrations over the North China Plain

Mingxu Liu[1], Xin Huang[2], Yu Song[1*], Tingting Xu[1], Shuxiao Wang[3], Zhijun Wu[1], Min Hu[1], Lin Zhang[4], Qiang Zhang[5], Yuepeng Pan[6], Tong Zhu[1]

[1]State Key Joint Laboratory of Environmental Simulation and Pollution Control, Department of Environmental Science, Peking University, Beijing 100871, China

[2]Joint International Research Laboratory of Atmospheric and Earth System Sciences, School of Atmospheric Sciences, Nanjing University, Nanjing, China

[3]State Key Joint Laboratory of Environmental Simulation and Pollution Control, School of Environment, Tsinghua University, Beijing 100084, China

[4]Laboratory for Climate and Ocean–Atmosphere Studies, Department of Atmospheric and Oceanic Sciences, School of Physics, Peking University, Beijing 100871, China

[5]Ministry of Education Key Laboratory for Earth System Modeling, Center for Earth System Science, Institute for Global Change Studies, Tsinghua University, Beijing 100084, China

[6]State Key Laboratory of Atmospheric Boundary Layer Physics and Atmospheric Chemistry (LAPC), Institute of Atmospheric Physics, Chinese Academy of Sciences, Beijing, China

Correspondence to: Yu Song (songyu@pku.edu.cn)

Abstract. The North China Plain has been identified as a significant hotspot of ammonia (NH_3) due to extensive agricultural activities. Satellite observations suggest a significant increase of about 30% in tropospheric gas-phase NH_3 concentrations in this area during 2008−2016. However, the estimated NH_3 emissions decreased slightly because of changes in Chinese agricultural practices, i.e., the transition in fertilizer types from ammonium carbonate fertilizer to urea, and in the livestock rearing system from free-range to intensive farming. We note that the emissions of sulfur dioxide (SO_2) have rapidly declined by 60% over recent few years. By integrating in situ measurement datasets, multi-year NH_3 emission inventories, and chemical transport model simulations, we demonstrate that the increases in NH_3 can be almost entirely attributable to this rapid SO_2 emission reduction. The annual average sulfate concentrations decreased by about 50%, which significantly weakened the formation of ammonium sulfate and increased the average proportions of gas phase NH_3 within the total NH_3 column concentrations from 26% (2008) to 37% (2016). Both the decreases in sulfate and increases in NH_3 concentrations

Atmos. Chem. Phys. Discuss., https://doi.org/10.5194/acp-2018-880
Manuscript under review for journal Atmos. Chem. Phys.
Discussion started: 5 September 2018

show highest values in summer, possibly because the formation of sulfate aerosols is more sensitive to SO_2 emission reductions in summer than in other seasons.

1 Introduction

Ammonia (NH_3) is considered the most important alkaline gas in the atmosphere. On both a global and regional scale, NH_3 is mostly emitted from agricultural activities, mainly including fertilization and livestock industry (Bouwman et al., 1997). Gas-phase NH_3 can react with ambient sulfuric and nitric acids to form ammonium sulfate/bisulfate and ammonium nitrate aerosols (SNA), which constitute a significant fraction of atmospheric fine particles ($PM_{2.5}$) associated with potential human health impacts (Pope et al., 2009; Seinfeld and Pandis, 2006). Ammonia and ammonium (NH_4^+) is ultimately deposited back to the earth surface, contributing to acid deposition and eutrophication (Asman, 1998; Behera et al., 2013; Pozzer et al., 2017).

As a major agricultural country, China is the world's largest emitter of NH_3, the amount of which (~10 Tg) exceeds the sum of those in Europe (~4.0 Tg) and North America (~4.0 Tg) (Huang et al., 2012; Bouwman et al., 1997; Paulot et al., 2014). Fertilizer application and livestock manure management contribute to nearly 90% of China's NH_3 emissions (Huang et al., 2012; Zhang et al., 2018). Until now, NH_3 emission has not been regulated by the Chinese government, although it may be a potentially important contributor to haze pollution in China.

The North China Plain (the spatial definition of this area is illustrated in Fig. S1) is a hotspot of NH_3 loadings, as revealed by satellite detection and in situ ground measurements (Clarisse et al., 2009; Pan et al., 2018). Interestingly, satellite observations over the past decade have shown an increase in tropospheric columns of gaseous NH_3 in this area (Warner et al., 2017). But no quantitative studies have been performed to explain it. A long-term bottom-up inventory indicated that NH_3 emissions in China have displayed a slightly decreasing tendency. During 2006−2016, ammonium bicarbonate for crop fertilization was replaced by urea fertilizer (its fraction of application increasing from 60 to 90% of all nitrogen fertilizers), and the traditional free-range livestock system was replaced by intensive animal rearing system (i.e., raising livestock in confinement at a high stocking density) in the livestock industry (increasing from 21% in 2006 to 48% in 2016; shown in

Table S1). These changes in agricultural practices have lowered the volatilization rates of NH_3 (Kang et al., 2016).

Through the widespread use of the flue gas desulfurization in power plants since 2000s in China, SO_2 emissions have gradually decreased (Lu et al., 2011; Li et al., 2010). Li et al. (2017) found it was reduced by 70% from the peak year (around 2006) to 2016 based on satellite observations and bottom up methods. Specifically, the initiation of the "Action Plan for Air Pollution Prevention and Control" (referred to as the national "Ten Measures for Air") since 2013 resulted in a rapid reduction of about 50% over recent few years, from ~30 Tg in 2012 to ~14 Tg in 2016 according to the Multi-resolution Emission Inventory for China (MEIC). To our knowledge, such a strong decrease in SO_2 emissions is only found in China. In contrast, emissions of nitrogen oxides (NO_x) in MEIC peaked around 2012 with only a moderate decrease of ~20% from 2012 to 2016 (Liu et al., 2016).

Here, we hypothesize that the rapid SO_2 emission reduction is the reason for the increase in tropospheric NH_3 concentrations over the North China Plain. To verify this, we first used observation datasets from the ground and space to infer the relationship between the trends in NH_3 and SO_2 concentrations. A comprehensive long-term NH_3 emission inventory, developed by our recent studies based on bottom-up methods, was also used to demonstrate the inter-annual variations of NH_3 emissions in this region. Then, we performed multi-year simulations with Weather Research and Forest model coupled with Chemistry (WRF-Chem) to test the impact of changes in SO_2 emissions on tropospheric NH_3 concentrations in terms of the magnitude and seasonal variation.

2 Methods

2.1 Observations datasets

Observations from space and ground stations were used in this study. Tropospheric vertical column densities (VCDs) of NH_3 were derived from the measurements of Infrared Atmospheric Sounding Interferometer (IASI) onboard MetOp-A (Van Damme et al., 2015; Clarisse et al., 2009; Van Damme et al., 2017). We determined the annual averages of NH_3 column concentrations over the North China Plain on a $0.25^o \times 0.25^o$ grid during 2008−2016, based on the relative error weighting mean method (Van Damme et al., 2014). The monthly NH_3 concentrations were measured using passive NH_3 diffusive

samplers (Analysts, CNR-Institute of Atmospheric Pollution, Roma, Italy) from September 2015 to August 2016 at 11 sites over Northern China (Pan et al., 2018). The SO_2 VCDs were provided by the ozone monitoring instrument (OMI) measurements to test the trend of SO_2 concentrations. They were derived from the daily level 3 data set OMSO2e, released by the NASA Goddard Earth Sciences Data and Information Services Center. Besides, daily $PM_{2.5}$ were sampled by quartz-fiber filters at an urban atmosphere environment monitoring station in Peking University (39.99 °N, 116.3 °E) of Beijing, China since 2013. The major water-soluble inorganic compounds (e.g., NH_4^+, NO_3^-, and SO_4^{2-}) were analyzed by ion-chromatography.

2.2 WRF-Chem simulations

In this study, the simulations with Weather Research and Forecast Model coupled Chemistry (Grell et al., 2005) version 3.6.1 (WRF-Chem) were conducted for the domain of North China Plain for the years 2008, 2010, 2012, 2014, 2015, and 2016 (referred to as Run_08−16). We ran the model with a horizontal resolution of 30 × 30 km and 24 vertical layers, extending from the surface to 50 hPa. The initial and boundary meteorological condition was derived from 6-h National Centers for Environmental Prediction reanalysis data. The detailed model configuration were described in our previous study (Huang et al., 2014). The anthropogenic emissions, including power plant, industrial, residential, and vehicle emissions, were derived from the MEIC (Multi-resolution Emission Inventory for China; available online at: http://www.meicmodel.org/) database. The MEIC data show that the annual SO_2 emissions in North China Plain were cut by about 60%, from 990 Gg in 2008 to 418 Gg in 2016.

2.3 NH_3 emission inventory

A high-resolution NH_3 emission inventory (1km×1km, month) was developed by our research group based on the bottom-up method. The emission factors were parameterized with regional farming practices, ambient temperature, soil pH and wind speeds etc. The full details can be found in our previous studies (Kang et al., 2016; Huang et al., 2012; Huo et al., 2015). The inventory had similar spatial features with recent satellite observations (Van Damme et al., 2014), and its amount is close to the emission estimated by the inversion model using ammonium wet deposition data (Paulot et al., 2014). Recent modeling

results also showed its good performance by comparing with ammonium observations in China (Huang et al., 2015). The inventories covered the period from 1980 to 2016 and considered the inter-annual variability in activity levels and agricultural practices. In the North China Plain, the increasing use of urea fertilizer (from 4.5 and 5.2 million tons) but decreased ammonium bicarbonate (from 1.5 to 0.4 million tons) led to a 20% reduction in NH_3 emissions from fertilizer application during 2008−2016 (Table S1). Meanwhile, although the number of some livestock animals increased slightly, the proportion of intensive animal rearing system increased to nearly half of the livestock industry in 2016, compared to 28% in 2008. The increased livestock animals raised but more effective manure management resulted in the livestock emissions in North China Plain remaining almost constant (around 115 Gg per year) (Table S1).

3 Results and Discussions

3.1 Trends in emissions and concentrations of NH_3 vs. SO_2

According to the Infrared Atmospheric Sounding Interferometer measurements, the North China Plain showed the highest VCDs of NH_3 in China, which mostly ranged from 15 to 30 $\times 10^{15}$ molecules/cm^2 during 2008−2014, and increased to above 30 $\times 10^{15}$ molecules/cm^2 in 2015 and 2016 (Fig. S1). We found the annual NH_3 column concentrations increased significantly ($P < 0.05$) over the North China Plain between 2008 and 2016 (Fig. 1a). The average tropospheric NH_3 columns first fluctuated between 2008 and 2013, and then rapidly increased from 21 $\times 10^{15}$ molecules/cm^2 in 2013 to 27 $\times 10^{15}$ molecules/cm^2 in 2016. It showed an overall increase of 30%, or an average annual increase of 0.9 $\times 10^{15}$ molecules cm^{-2} yr^{-1}. Seasonally, the increase in NH_3 columns was more pronounced in summertime (June−August, JJA), with an annual increase rate of 1.8×10^{15} molecules/cm^2 between 2008 and 2016, which was much higher than in other seasons (< 1×10^{15} molecules/cm^2).

In contrast to the trends in tropospheric NH_3 concentrations, the NH_3 emissions (developed based on the methods by Kang et al. (2016)) first experienced a decreasing tendency from 2008 to 2011 (300 Gg in 2009 to 275 Gg in 2011), and then remained constant at around 280 Gg during 2011−2016 over the North China Plain, representing a slight decrease (Fig. 1b). As aforementioned, the changes in fertilizer use and livestock rearing practices have lowered NH_3 emission rates. Overall,

the NH_3 emissions cannot track the upward trend of tropospheric NH_3 concentrations.

During 2008−2016, SO_2 column concentrations were subject to a dramatic decline ($P < 0.01$) due to a 60% decrease in SO_2 emissions (derived from the MEIC database). The annual mean SO_2 VCDs reduced from 14×10^{15} molecules/cm^2 (2008) to 4×10^{15} molecules/cm^2 (2016), showing a percent reduction of nearly 70%. Especially during 2012−2016, the decreases in SO_2 emissions and VCDs accelerated owing to the implementation of the "Action Plan for Air Pollution Prevention and Control" by the Chinese government. In situ ground measurements in a typical urban station in the North China Plain indicated that the annual average sulfate concentration (SO_4^{2-}) in $PM_{2.5}$ decreased by 35% (2013−2016) along with rapid SO_2 reductions, which was accompanied by a 33% decrease of particulate ammonium (NH_4^+) (Fig. 1b). The decrease in SO_4^{2-} during summertime (JJA) reached 60%, which was much higher than in other seasons.

3.2 Simulations of increasing trend in NH_3 columns

We first evaluated WRF-Chem model results against measurements of surface NH_3 concentrations available in North China Plain as well as the satellite-retrieved NH_3 columns. The simulated monthly averaged surface NH_3 concentrations at 11 in situ stations (mean + standard deviation: 13.5 ± 6.8 μg/m^3) generally agreed with corresponding observations (13.4 ± 9.7 μg/m^3) with a correlation coefficient of 0.57. More than 70% of the comparisons differed within a factor of two (Fig. 2). Both simulations and observations show high NH_3 concentrations of about 30 μg/m^3 in warm seasons (March-October) due to enhanced NH_3 volatilization and frequent fertilization activities, and lower values (mostly < 15 μg/m^3) in other months (Fig. 3). Spatially, the hotpot of NH_3 was mainly concentrated in Hebei, Shandong and Henan provinces, which had the most intensive agricultural productions over China and thus emitted considerable gas-phase NH_3 into atmosphere. We note that the simulated NH_3 concentrations were underestimated by about a factor of two in wintertime (January, February, and December). Recently, NH_3 emission from the residential coal and biomass combustion for heating is considered to be a potentially important source of NH_3 in suburban and rural areas during wintertime (Li et al., 2016), but it has been not fully included in our bottom-up inventory, which could be responsible for such deviation between the model and observations.

The simulated NH_3 VCDs, calculated by integrating NH_3 molecular concentrations from the surface level to top troposphere, was consistent with observed NH_3 columns of 2016 on the magnitude and spatial-temporal patterns, although

the winter results were underestimated (Fig. S2). Both IASI measurements and the WRF-Chem simulation showed high annual mean NH_3 column concentrations in Hebei, Shandong and Henan provinces, reaching above 30×10^{15} molecules/cm^2. Moreover, we also evaluated the modelled SNA concentrations using the filter-based $PM_{2.5}$ samples at an urban atmospheric monitoring station in North China Plain during 2014−2016 (Fig. S3). The model generally reproduced the observed SNA concentrations, with small annual mean bias for sulfate (−2%) and ammonium (−13%) and a relatively large bias for nitrate (−24%). Overall, the model performed well in modelling the concentrations in tropospheric NH_3 as well as secondary inorganic aerosols, which provides high confidence for the following interpretation of the NH_3 increases.

The model successfully reproduced the observed increasing trend in NH_3 columns over the North China Plain during 2008−2016 (Fig. 4). The modelled NH_3 columns were systemically lower than the measurements because the relative error weighting mean method would bias a high result due to the smaller relative error in a larger column (Van Damme et al., 2014; Whitburn et al., 2016). Similar to IASI observations, an increase of 25% in NH_3 columns was found in the simulations between 2012 and 2016, and the SO_2 columns averaged over the North China Plain decreased by 50% in this period, both of which were close to the measurements.

To verify our hypothesis, we replaced SO_2 emissions during 2010−2016 by those in 2008, and repeated the simulations (referred to as Run_10_S08 to Run_16_S08). It was noticeable that under these conditions, the increasing trend of NH_3 column concentrations disappeared, and even a slight decrease took place (Fig. 4). The largest difference was found in 2015 and 2016, when the annual NH_3 columns were reduced by about 40%, or 10×10^{15} molecules/cm^2, corresponding to the 60% reduction in SO_2 emissions between 2008 and 2016. These tests support our hypothesis that the rapid SO_2 emission reductions led to the increased NH_3 levels during 2008−2016.

3.3 Influence of SO_2 emission reductions on tropospheric NH_3 concentrations

As we indicated above, SO_4^{2-} was observed to be decreasing over recent years in response to the reductions of SO_2 emissions. This was also reproduced by our simulations, which showed that the annual average sulfate concentrations decreased by almost 50% in the lower troposphere. This decreasing trend was especially pronounced after 2013 owing to the much effective SO_2 emission reductions. Given that the vapor pressure of H_2SO_4(g) is practically zero over atmospheric

particles, atmospheric SO_4^{2-} is predominately in the particle phase and can combine with NH_3 available in air, forming sulfate salts (mostly ammonium sulfate/bisulfate) (Seinfeld and Pandis, 2006). Since North China Plain is typically under rich NH_3 regimes, SO_4^{2-} is mainly in the form of ammonium sulfate (Meng et al., 2011; Huang et al., 2017); and the aforementioned SO_4^{2-} reductions would therefore increase atmospheric NH_3 concentrations by driving the phase state of NH_3 from particulate to gaseous.

By assuming that a 1 mol decrease in simulated SO_4^{2-} would lead to a 2 mol increase in ambient gaseous NH_3 in this region, the average annual increase in the tropospheric NH_3 columns due to the reductions of SO_4^{2-} was estimated to be approximately 1.5×10^{15} molecules cm^{-2} yr^{-1} over North China Plain during 2008−2016, which is comparable with or higher than the simulated results from Run_08 to Run_16, as well as the IASI observations (0.9×10^{15} molecules cm^{-2} yr^{-1}). By neglecting the deposition processes, we found that the rapid SO_2 emission reduction of 50% from 2012 to 2016 could result in a 55% increase in the NH_3 columns, compared to that of 30% recorded by IASI observations. Overall, the estimation results confirmed that the increasing trend of NH_3 can be entirely attributable to the SO_2 emission reductions.

We compared the spatial patterns of decreased SO_4^{2-} and increased NH_3 between 2008 and 2016 (Run_08 – Run_16). Large reductions of $6-10 \times 10^{15}$ molecules/cm^2 in annual averages of sulfate columns were concentrated in Hebei, Shandong and Henan provinces, the area subject to high SO_2 loadings and stringent emission controls (Fig. 5a). Meanwhile, the simulated increases in NH_3 columns reached more than 8×10^{15} molecules/cm^2 in most parts of the North China Plain (Fig. 5b), and were comparable with those observed by the IASI ($8-16 \times 10^{15}$ molecules/cm^2). In addition, we found that NH_4^+ concentrations have decreased with a similar magnitude to the increases in gas-phase NH_3 levels between Run_08 and Run_16. The proportion of NH_3 in the total (NH_3 + NH_4^+) increased on average from 26% in 2008 to 37% in 2016 over North China Plain. Figure 5c, d illustrated that without the large SO_2 emission reductions between 2008 and 2016 (i.e., replacing SO_2 emissions in 2016 by those in 2008, Run_08 – Run_16_S08), the sulfate columns partly increased, and correspondingly the NH_3 columns remained constant or decreased by about 5×10^{15} molecules/cm^2 (~20% relative to the 2008 level) in parts of the North China Plain. Thus, the increase in the tropospheric NH_3 columns was the result of a transition in NH_3 phase partitioning, which was associated with the decreased formation of ammonium sulfate due to SO_2 emission reductions.

Atmos. Chem. Phys. Discuss., https://doi.org/10.5194/acp-2018-880
Manuscript under review for journal Atmos. Chem. Phys.
Discussion started: 5 September 2018

Atmospheric Chemistry and Physics Discussions

The seasonal variations in SO_4^{2-} decreases and NH_3 increases were almost consistent (Fig. 6). We can see that the reduction of sulfate column concentrations between the Run_08 and Run_16 reached 1.3×10^{15} molecules/cm^2 in summer (JJA), which was about three times larger than in other seasons. The corresponding percent reductions ranged from 15% in DJF to 36% in JJA. Considering that the SO_2 emission reductions were uniform throughout the year, this seasonal pattern was likely attributed to the conversion efficiency of SO_2 to H_2SO_4. Our simulations showed that a 1 mol decrease in SO_2 corresponded to an approximately 0.7 mol decrease in particulate sulfate in summer over North China Plain, but the values dropped to below 0.4 in other seasons. It is known that the photochemical oxidation of SO_2 by OH radical is most active in summertime due to high atmospheric oxidizing capacity, and it dominates the formation of SO_4^{2-}, which could make the response of SO_4^{2-} concentrations to SO_2 emission reductions more sensitive (Paulot et al., 2017; Huang et al., 2014). The comparison of modelled NH_3 columns also showed a markedly higher increase in summer months than during other seasons, driven by the variations in SO_4^{2-}. Furthermore, by comparing the model results between the Run_16 and Run_16_S08 cases, we found that without considering the SO_2 emission reductions, the seasonal increases in NH_3 columns and decreases in SO_4^{2-} concentrations disappeared.

In addition, we noted that the simulated particulate nitrate (NO_3^-) concentrations appear to increase in the North China Plain between 2008 and 2016 despite a 23% reduction in NO_x emissions (Fig. S4). The in situ measurements in Beijing indicated that the NO_3^- concentrations fluctuated during 2013−2016. It implied that the NO_x emission reduction could not be responsible for the increase in NH_3. We also tested the effects of meteorological conditions on NH_3 variations by a simulation with meteorological fields in 2016 and anthropogenic emissions in 2012 (Run_16_E12). Compared to the Run_12 case, we found the change in meteorological fields (2012 vs. 2016) had a negligible influence on NH_3 concentrations in most of North China Plain. Although temperature increase was reported to partly contribute to the positive trend of NH_3 (Warner et al., 2017; Fu et al., 2017), our simulations indicated that the overall meteorological factors could not explain the observed significant increase tropospheric NH_3 concentrations over North China Plain.

4 Conslusion

In this study, we found that an increase in tropospheric NH_3 columns observed over the North China Plain during 2008−2016

was not caused by the increase in NH_3 emission, which actually displayed a slightly decreasing tendency. Neither meteorological conditions nor NOx emissions could explain it. Our work strongly indicates that the rapid SO_2 emission reductions (60%) from 2008 to 2016 were responsible for almost the entire NH_3 increases. The SO_2 emissions reduction decreased SO_4^{2-} concentrations by about 50% in the lower troposphere, which reduced the formation of ammonium sulfate particles and consequently increased the average proportions of gas phase NH_3 from 26% (2008) to 37% (2016) within the total NH_3 column concentrations. The transition in the NH_3 phase state from particulate to gaseous was more pronounced in summertime than in other seasons, due to a more sensitive response of SO_4^{2-} concentrations to SO_2 emission reductions.

Given the on-going stringent controls on SO_2 emissions in China, a continued increase in NH_3 concentrations is anticipated if NH_3 emissions are not well-regulated. The increased tropospheric NH_3 levels may have a significant impact on air pollution and nitrogen deposition in China. For instance, the elevated NH_3 would facilitate ammonium nitrate formation based on the aerosol thermodynamic equilibrium and negatively impact $PM_{2.5}$ control. That is supported by the fact that NO_3^- concentrations remain high in Northern China and have become increasingly important in contributing to $PM_{2.5}$ pollution (Wen et al., 2018; Li et al., 2018), despite a moderate NO_x emission reduction. The increased proportion of gas-phase NH_3 within the total can increase ammonium-nitrogen deposition since gas-phase ammonia deposits more rapidly than particle ammonium. This may alter the spatial pattern of regional nitrogen deposition with higher levels of NH_3 deposited near emission sources. These effects are important for human and ecosystem health and need to be investigated in future studies.

Data availability. NH_3 vertical column density data are freely available through the AERIS database: http://iasi.aeris-data.fr/NH3/. The SO_2 vertical column density retrieved from the Ozone Monitoring Instrument is available from Level-3 Aura/OMI Global OMSO2e Data Products released by NASA Goddard Earth Science Data and Information Service Center (https://disc.sci.gsfc.nasa.gov/). Anthropogenic emissions in industry, power plants, transportation, and residential sectors are obtained from Multi-resolution Emission Inventory for China (MEIC, http://www.meicmodel.org/).

Author contributions. Y.S., M.H., and T.Z. designed the study. Z.W. and M.H. conducted in situ measurements of aerosol

chemical compositions. Y.P. conducted in situ measurements of gas-phase ammonia concentrations. Q.Z. developed the MEIC emission database. M.L. and X.H. contributed to the development of ammonia emission inventory. M.L., X.H., Y.S., S.W., L.Z and T.Z. analyzed data. M.L. led the writing with input from all co-authors.

Competing interests. The authors declare that they have no conflict of interest.

Acknowledgments. This study was supported by National Natural Science Foundation of China (NSFC) (91644212).

References

Asman, W. A. H.: Ammonia:emission, atmospheric transport and depostion, New Phytologist, 139, 1998.

Behera, S. N., Sharma, M., Aneja, V. P., and Balasubramanian, R.: Ammonia in the atmosphere: a review on emission sources, atmospheric chemistry and deposition on terrestrial bodies, Environmental science and pollution research international, 20, 8092-8131, 10.1007/s11356-013-2051-9, 2013.

Bouwman, A. F., Lee, D. S., Asman, W. A. H., Dentener, F. J., Van Der Hoek, K. W., and Olivier, J. G. J.: A global high-resolution emission inventory for ammonia, Global Biogeochem. Cy., 11, 561-587, 10.1029/97gb02266, 1997.

Clarisse, L., Clerbaux, C., Dentener, F., Hurtmans, D., and Coheur, P.-F.: Global ammonia distribution derived from infrared satellite observations, Nat. Geosci., 2, 479-483, 10.1038/ngeo551, 2009.

Fu, X., Wang, S., Xing, J., Zhang, X., Wang, T., and Hao, J.: Increasing Ammonia Concentrations Reduce the Effectiveness of Particle Pollution Control Achieved via SO2 and NOX Emissions Reduction in East China, Environ. Sci. Tech. let., 4, 221–227, 10.1021/acs.estlett.7b00143, 2017.

Grell, G. A., Peckham, S. E., Schmitz, R., McKeen, S. A., Frost, G., Skamarock, W. C., and Eder, B.: Fully coupled "online" chemistry within the WRF model, Atmos. Environ., 39, 6957-6975, 10.1016/j.atmosenv.2005.04.027, 2005.

Huang, X., Song, Y., Li, M., Li, J., Huo, Q., Cai, X., Zhu, T., Hu, M., and Zhang, H.: A high-resolution ammonia emission inventory in China, Global Biogeochem. Cy., 26, GB1030, 10.1029/2011GB004161, 2012.

Huang, X., Song, Y., Zhao, C., Li, M., Zhu, T., Zhang, Q., and Zhang, X.: Pathways of sulfate enhancement by natural and anthropogenic mineral aerosols in China, J. Geophys. Res. Atmos., 119, 14,165-114,179, 10.1002/2014JD022301, 2014.

Huang, X., Song, Y., Zhao, C., Cai, X., Zhang, H., and Zhu, T.: Direct Radiative Effect by Multicomponent Aerosol over China, J. Climate, 28, 3472-3495, doi:10.1175/JCLI-D-14-00365.1, 2015.

Huang, X., Liu, Z., Liu, J., Hu, B., Wen, T., Tang, G., Zhang, J., Wu, F., Ji, D., Wang, L., and Wang, Y.: Chemical characterization and source identification of PM2.5 at multiple sites in the Beijing–Tianjin–Hebei region, China, Atmos. Chem. Phys., 17, 12941-12962, 10.5194/acp-17-12941-2017, 2017.

Huo, Q., Cai, X., Kang, L., Zhang, H., Song, Y., and Zhu, T.: Estimating ammonia emissions from a winter wheat cropland in North China Plain with field experiments and inverse dispersion modeling, Atmos. Environ., 104, 1-10, 10.1016/j.atmosenv.2015.01.003, 2015.

Kang, Y., Liu, M., Song, Y., Huang, X., Yao, H., Cai, X., Zhang, H., Kang, L., Liu, X., Yan, X., He, H., Zhang, Q., Shao, M., and Zhu, T.: High-resolution ammonia emissions inventories in China from 1980 to 2012, Atmos. Chem. Phys., 16, 2043-2058, 10.5194/acp-16-2043-2016, 2016.

Li, C., Zhang, Q., Krotkov, N. A., Streets, D. G., He, K., Tsay, S.-C., and Gleason, J. F.: Recent large reduction in sulfur dioxide emissions from Chinese power plants observed by the Ozone Monitoring Instrument, Geophys. Res. Lett., 37, L08807, 10.1029/2010gl042594, 2010.

Li, C., McLinden, C., Fioletov, V., Krotkov, N., Carn, S., Joiner, J., Streets, D., He, H., Ren, X., Li, Z., and Dickerson, R. R.: India Is Overtaking China as the World's Largest Emitter of Anthropogenic Sulfur Dioxide, Scientific reports, 7, 14304, 10.1038/s41598-017-14639-8, 2017.

Li, H., Zhang, Q., Zheng, B., Chen, C., Wu, N., Guo, H., Zhang, Y., Zheng, Y., Li, X., and He, K.: Nitrate-driven urban haze pollution during summertime over the North China Plain, Atmos. Chem. Phys., 18, 5293-5306, 10.5194/acp-18-5293-2018, 2018.

Li, Q., Jiang, J., Cai, S., Zhou, W., Wang, S., Duan, L., and Hao, J.: Gaseous Ammonia Emissions from Coal and Biomass Combustion in Household Stoves with Different Combustion Efficiencies, Environ. Sci. Tech. let., 3, 98-103, 10.1021/acs.estlett.6b00013, 2016.

Liu, F., Zhang, Q., van der A, R. J., Zheng, B., Tong, D., Yan, L., Zheng, Y., and He, K.: Recent reduction in NOx emissions over China: synthesis of satellite observations and emission inventories, Environ. Res. Lett., 11, 114002, 10.1088/1748-9326/11/11/114002, 2016.

Lu, Z., Zhang, Q., and Streets, D. G.: Sulfur dioxide and primary carbonaceous aerosol emissions in China and India, 1996–2010, Atmos. Chem. Phys., 11, 9839-9864, 10.5194/acp-11-9839-2011, 2011.

Meng, Z. Y., Lin, W. L., Jiang, X. M., Yan, P., Wang, Y., Zhang, Y. M., Jia, X. F., and Yu, X. L.: Characteristics of atmospheric ammonia over Beijing, China, Atmos. Chem. Phys., 11, 6139-6151, 10.5194/acp-11-6139-2011, 2011.

Pan, Y., Tian, S., Zhao, Y., Zhang, L., Zhu, X., Gao, J., Huang, W., Zhou, Y., Song, Y., Zhang, Q., and Wang, Y.: Identifying Ammonia Hotspots in China Using a National Observation Network, Environmental science & technology, 52, 3926-3934, 10.1021/acs.est.7b05235, 2018.

Paulot, F., Jacob, D. J., Pinder, R. W., Bash, J. O., Travis, K., and Henze, D. K.: Ammonia emissions in the United States, European Union, and China derived by high-resolution inversion of ammonium wet deposition data: Interpretation with a new agricultural emissions inventory (MASAGE_NH3), J. Geophys. Res. Atmos., 119, 4343-4364, 10.1002/2013jd021130, 2014.

Paulot, F., Fan, S., and Horowitz, L. W.: Contrasting seasonal responses of sulfate aerosols to declining SO2 emissions in the Eastern U.S.: Implications for the efficacy of SO2 emission controls, Geophys. Res. Lett., 44, 455-464, 10.1002/2016gl070695, 2017.

Pope, C. A. I., Ezzati , M., and Dockery , D. W.: Fine-Particulate Air Pollution and Life Expectancy in the United States, N. Engl. J. Med., 360, 376-386, doi:10.1056/NEJMsa0805646, 2009.

Pozzer, A., Tsimpidi, A. P., Karydis, V. A., de Meij, A., and Lelieveld, J.: Impact of agricultural emission reductions on fine-particulate matter and public health, Atmos. Chem. Phys., 17, 12813-12826, 10.5194/acp-17-12813-2017, 2017.

Seinfeld, J. H., and Pandis, S. N.: Atmospheric Chemistry and Physics: From Air Pollution to Climate Change, 2nd ed., JOHN WILEY & SONS, 2006.

Van Damme, M., Clarisse, L., Heald, C. L., Hurtmans, D., Ngadi, Y., Clerbaux, C., Dolman, A. J., Erisman, J. W., and Coheur, P. F.: Global distributions, time series and error characterization of atmospheric ammonia (NH3) from IASI satellite observations, Atmos. Chem. Phys., 14, 2905-2922, 10.5194/acp-14-2905-2014, 2014.

Van Damme, M., Clarisse, L., Dammers, E., Liu, X., Nowak, J. B., Clerbaux, C., Flechard, C. R., Galy-Lacaux, C., Xu, W., Neuman, J. A., Tang, Y. S., Sutton, M. A., Erisman, J. W., and Coheur, P. F.: Towards validation of ammonia (NH3) measurements from the IASI satellite, Atmospheric Measurement Techniques, 8, 1575-1591, 10.5194/amt-8-1575-2015, 2015.

Van Damme, M., Whitburn, S., Clarisse, L., Clerbaux, C., Hurtmans, D., and Coheur, P.-F.: Version 2 of the IASI NH3 neural network retrieval algorithm: near-real-time and reanalysed datasets, Atmospheric Measurement Techniques, 10, 4905-4914, 10.5194/amt-10-4905-2017, 2017.

Warner, J. X., Dickerson, R. R., Wei, Z., Strow, L. L., Wang, Y., and Liang, Q.: Increased atmospheric ammonia over the world's major agricultural areas detected from space, Geophys. Res. Lett., 44, 2875-2884, 10.1002/2016gl072305, 2017.

Wen, L., Xue, L., Wang, X., Xu, C., Chen, T., Yang, L., Wang, T., and Wang, W.: Summertime fine particulate nitrate pollution in the North China Plain: Increasing trends, formation mechanisms, and implications for control policy, Atmos. Chem. Phys. Discuss., 2018, 1-27, 10.5194/acp-2018-89, 2018.

Whitburn, S., Van Damme, M., Clarisse, L., Bauduin, S., Heald, C. L., Hadji-Lazaro, J., Hurtmans, D., Zondlo, M. A., Clerbaux, C., and Coheur, P. F.: A flexible and robust neural network IASI-NH3retrieval algorithm, J. Geophys. Res. Atmos., 121, 6581-6599, 10.1002/2016jd024828, 2016.

Zhang, L., Chen, Y., Zhao, Y., Henze, D. K., Zhu, L., Song, Y., Paulot, F., Liu, X., Pan, Y., Lin, Y., and Huang, B.: Agricultural ammonia emissions in China: reconciling bottom-up and top-down estimates, Atmos. Chem. Phys., 18, 339-355, 10.5194/acp-18-339-2018, 2018.

Atmos. Chem. Phys. Discuss., https://doi.org/10.5194/acp-2018-880
Manuscript under review for journal Atmos. Chem. Phys.
Discussion started: 5 September 2018

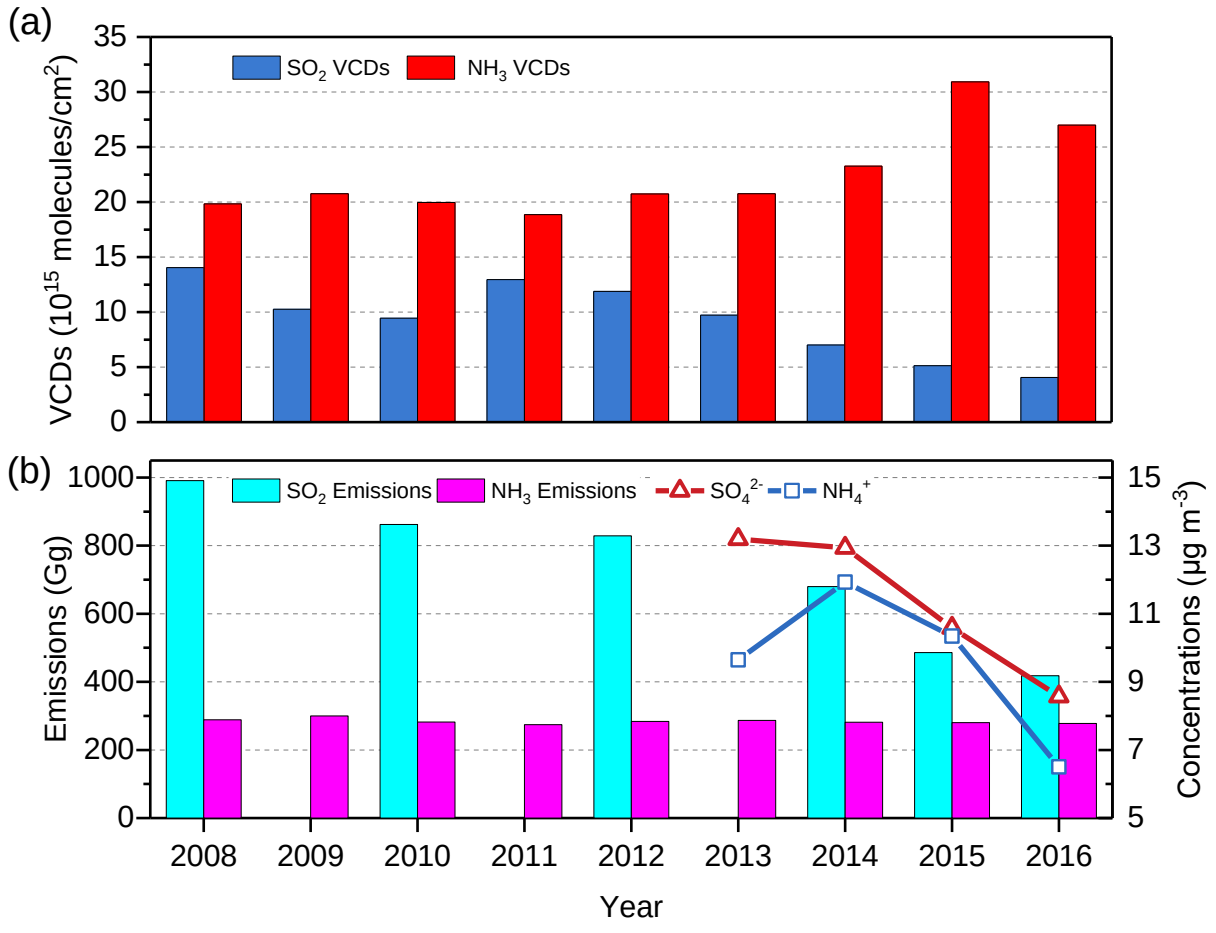

Figure 1. (a) Inter-annual trends of SO_2 and NH_3 VCDs averaged over North China Plain from 2008 to 2016. (b) Inter-annual trends of emissions of SO_2 and NH_3 from 2008 to 2016, and mean concentrations of $PM_{2.5}$ sulfate and ammonium derived from in situ measurements at an urban station (Beijing, 39.99 °N, 116.3 °E) in North China Plain from 2013 to 2016.

Atmos. Chem. Phys. Discuss., https://doi.org/10.5194/acp-2018-880
Manuscript under review for journal Atmos. Chem. Phys.
Discussion started: 5 September 2018

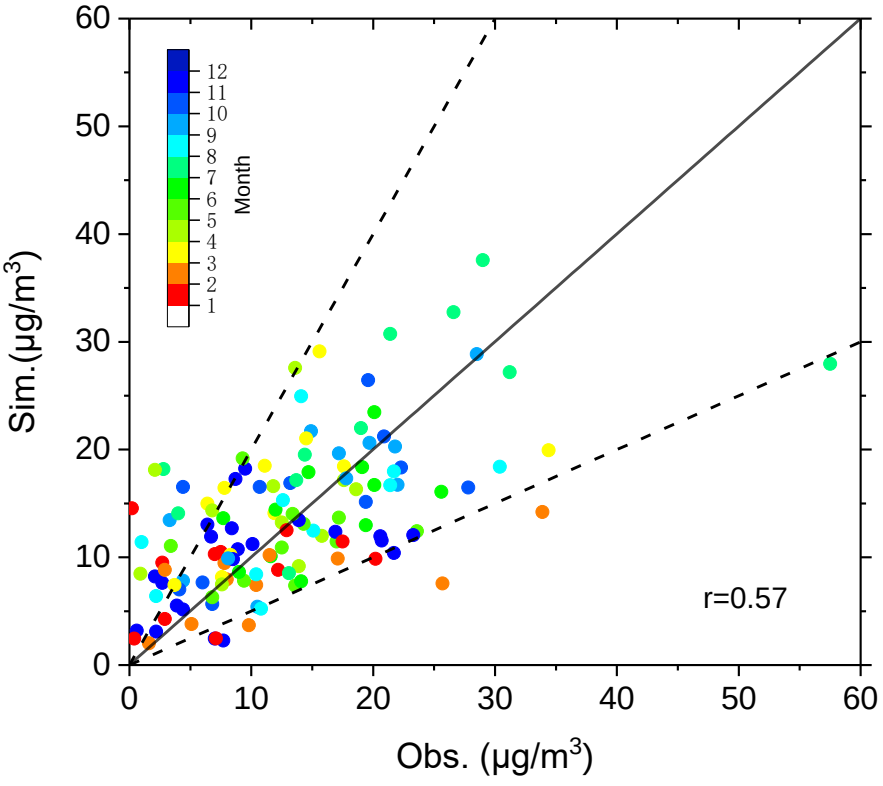

Figure 2. Comparison of modelled gaseous NH_3 concentrations with corresponding monthly measurements of NH_3 from Sep. 2015 to Aug. 2016. The 1:2 and 2:1 dashed lines are shown for reference and the Pearson correlation coefficient is shown inset.

Atmos. Chem. Phys. Discuss., https://doi.org/10.5194/acp-2018-880
Manuscript under review for journal Atmos. Chem. Phys.
Discussion started: 5 September 2018

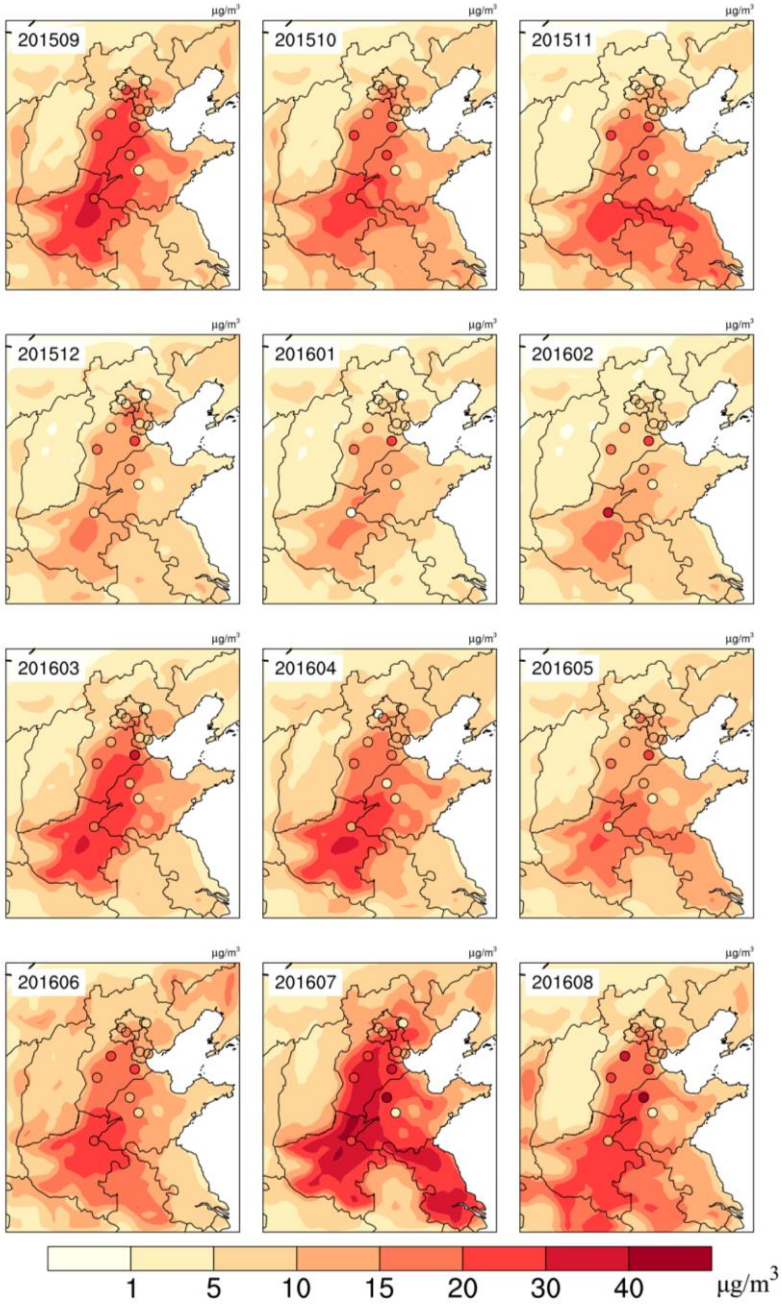

Figure 3. Spatial distribution of modelled surface NH_3 concentrations ($\mu g/m^3$) and in situ measurements over North China Plain from September, 2015 (201509) to August, 2016 (201608). The location of the North China Plain can be found in Fig. S1.

Atmos. Chem. Phys. Discuss., https://doi.org/10.5194/acp-2018-880
Manuscript under review for journal Atmos. Chem. Phys.
Discussion started: 5 September 2018

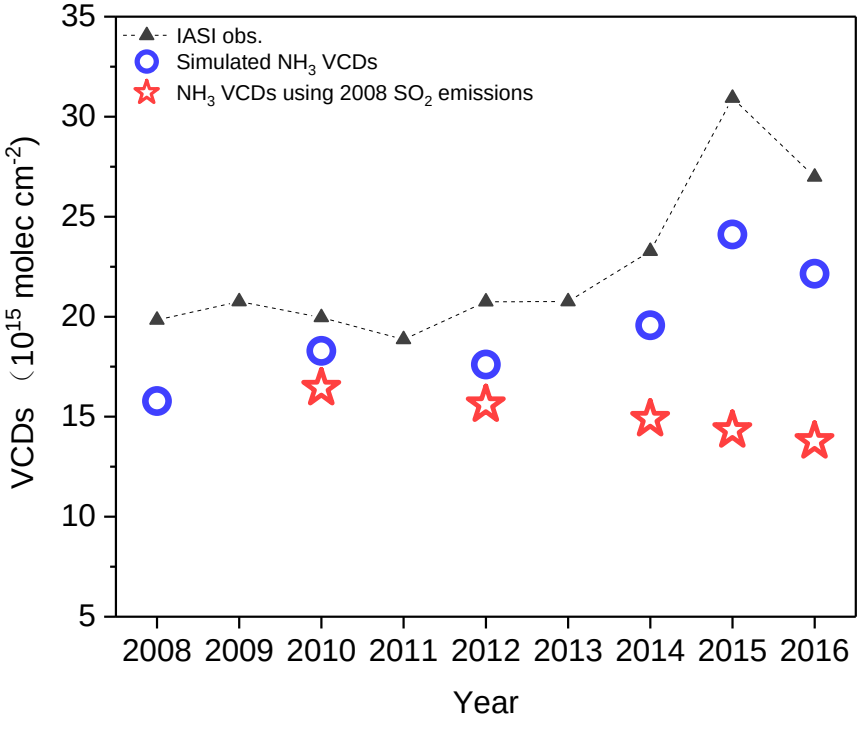

Figure 4. Trends in the annual averages of observed and simulated NH_3 columns. The red stars denote the simulated NH_3 columns under the 2008 SO_2 emissions levels (i.e., Run_10_S08 to Run_16_S08).

Atmos. Chem. Phys. Discuss., https://doi.org/10.5194/acp-2018-880
Manuscript under review for journal Atmos. Chem. Phys.
Discussion started: 5 September 2018

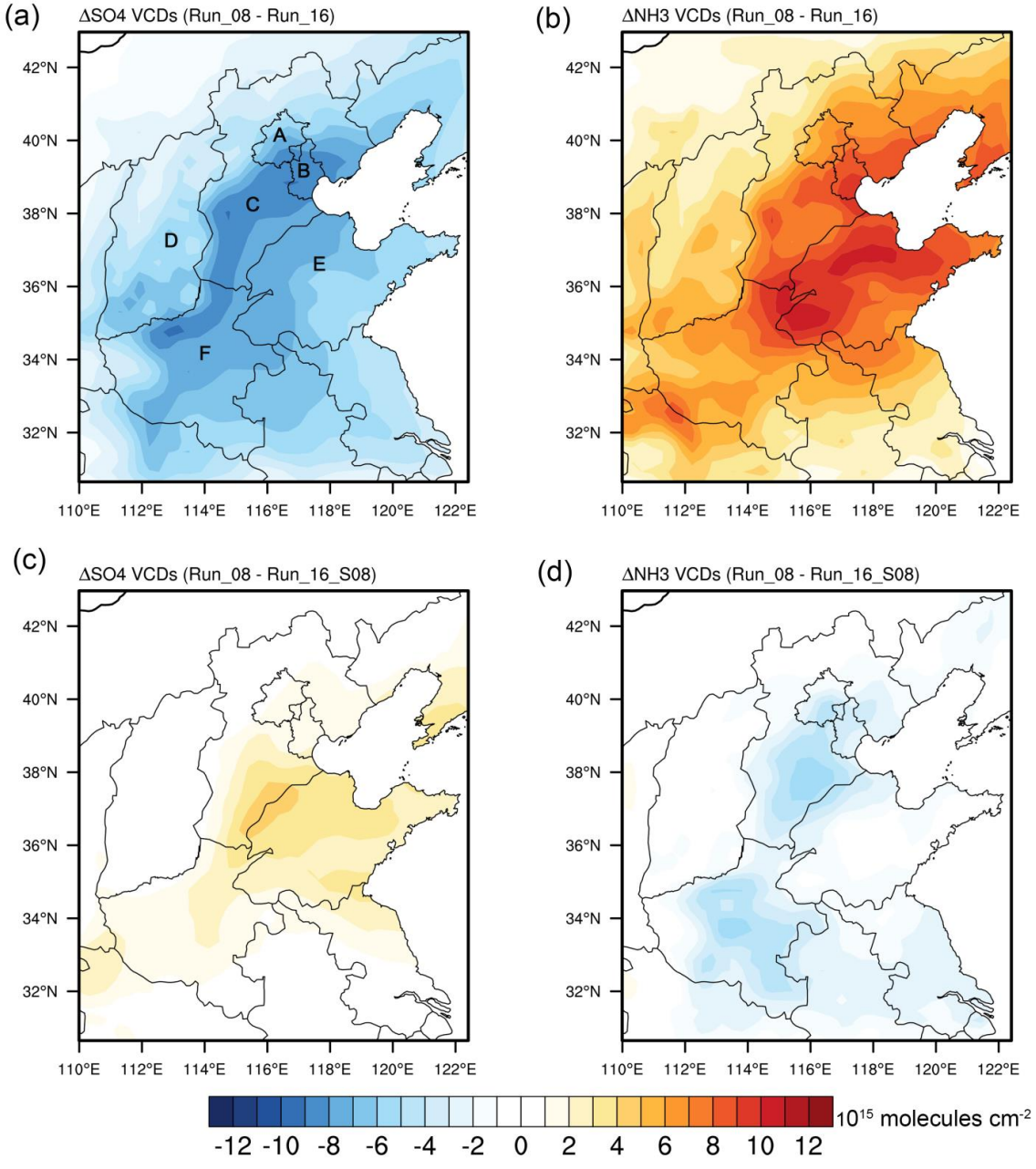

Figure 5. The differences between Run_08 and Run_16 (a, b), and between Run_08 and Run_16_S08 (c, d). A-F in Figure. 3a denote Beijing, Tianjin, Hebei, Shanxi, Shandong, and Henan Provinces, respectively.

Atmos. Chem. Phys. Discuss., https://doi.org/10.5194/acp-2018-880
Manuscript under review for journal Atmos. Chem. Phys.
Discussion started: 5 September 2018

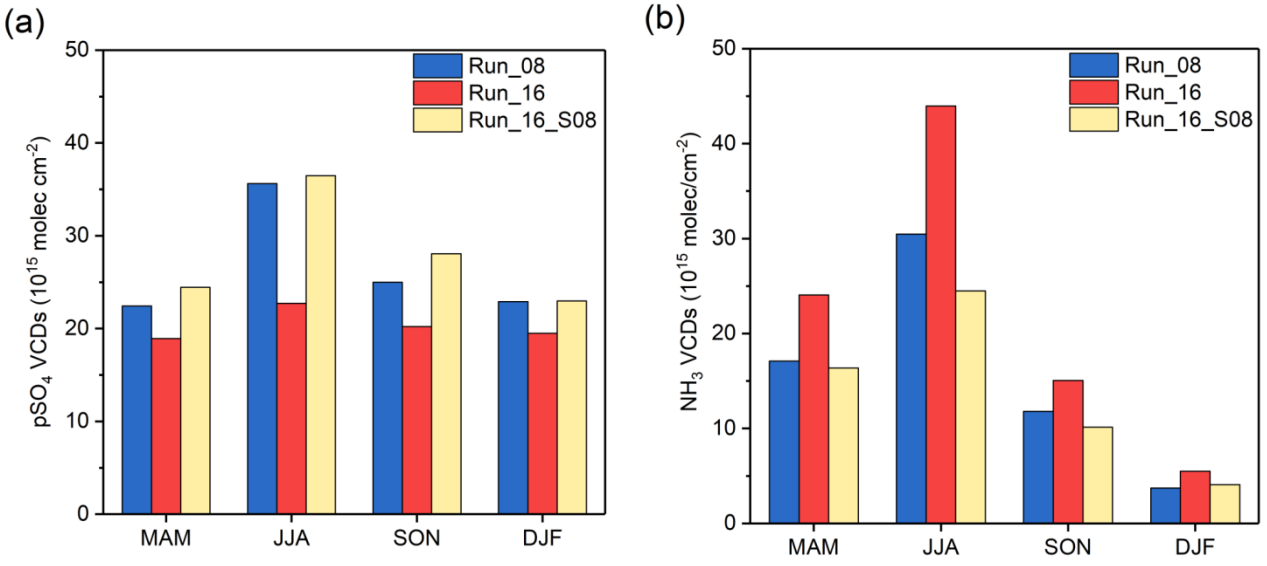

Figure 6. Seasonal patterns of simulated SO_4^{2-} (a) and NH_3 (b) columns for Run_08, Run_16, and Run_16_S08 (the simulation for 2016 with SO_2 emissions in 2008) cases. MAM, JJA, SON and DJF represent spring (Mar., Apr. and May), summer (Jun., Jul. and Aug.), autumn (Sep., Oct. and Nov.) and winter (Dec. Jan. and Feb.) months for this region.